
Hydrodynamic Modelling on Transport, Dispersion and Deposition of Suspended Particulate Matter in Pangani Estuary, Tanzania

Siajali Pamba, Yohana W. Shaghude, and Alfred N.N. Muzuka

Abstract

The present study was formulated with the aim of using MIKE 21 software in studying the hydrodynamic regime of the Pangani estuary. Water level, river discharge and wind drag force were used as hydrodynamic forcing factors during the model set up. The data set for the model (i.e. water level, tidal current winds and river discharge) were collected in Pangani estuary during the field campaigns conducted from December 2010 and August 2011. The results indicated that the tidal currents were relatively sluggish (0–0.05 m/s) in the beginning of model simulation. The ebb currents were established from 2 to 7 hours; originating from the inner part of the estuary tended to flow radially (Eastwards, Northwards and Southwards) soon after reaching the river mouth. The radial flow pattern of the ebb tidal currents seemed to be influenced by the funnel shape of the estuary. The flood tidal currents were established after 7 hours. The flood tidal phase started earlier on the southern part of the river mouth compared to the northern and tended to become more intensive on the northern part than on the southern part of the estuary. The currents pattern observed were influencing the transport and deposition of Suspended Particulate Matter (SPM). The maximum deposition of SPM preferentially occurred about 3 km north and south of the estuary mouth and the minimum deposition occurred in the middle of the estuary mouth. The deposition of SPM was highest during the southeast monsoon relative to the northeast monsoon. Approximately 872.6 kg/m²/year of SPM were brought into the estuary. This implies that, in the long term, the SPM deposition along the river mouth will significantly change the Pangani hydrodynamic regime, from its present condition. Also infilling of navigational channel and alteration of the ecosystems is imminent. Urgent actions are required to minimize the generation of SPM within the Pangani river basin.

Keywords

Hydrodynamic modelling • Suspended particulate matter • Pangani estuary

S. Pamba (✉)

Department of Aquatic Sciences and Fisheries Technology, College of Agricultural Sciences and Fisheries Technology, University of Dar es Salaam, 60091 Dar es Salaam, Tanzania
e-mail: engpambasi@yahoo.co.uk

Y.W. Shaghude

Institute of Marine Sciences, University of Dar es Salaam, 668 Zanzibar, Tanzania
e-mail: yohana.shaghude@gmail.com; shaghude@ims.udsm.ac.tz

A.N.N. Muzuka

Nelson Mandela African Institute of Science and Technology, 447 Arusha, Tanzania
e-mail: alfred.muzuka@nm-aist.ac.tz

Introduction

The use of hydrodynamic models have been successfully applied in investigating engineering and environmental problems; including bathymetric charting (Long 2009), prediction of tides (Kregting and Elsaber 2014) transport and dispersion of pollutants (Gerritsen et al. 2000; Zhen-Gang 2008), prediction of oil dispersion pathway (Gritfull et al. 2009), eutrophication, assessing flood risk (Ghimire 2013; Timbadiya et al. 2013) and transport of suspended particulate matter (SPM) (Comerma et al. 2002; Hu et al. 2009). Due to their wide range of applicability, hydrodynamic models are therefore considered as useful tools for studying dispersion and transport of SPM in complex coastal systems (Kregting and Elsaber 2014). Estuaries which are defined as “semi-enclosed coastal water bodies which have free connections with the open seas and within which the salinity of the water is measurably different from the salinity of the open sea (Carmeron and Pritchard 1963; Cuff and Tomczak 1983; Priya et al. 2012)” are considered to be hydrodynamically complex coastal systems.

Estuaries are typically characterized by their strong gradients of water surface level, salinity, water temperature and suspended sediment concentration (Duck and Wewetzer 2001; Priya et al. 2012; Jay et al. 2014). Estuaries act as a transition zone between the upland wetlands and the ocean, and they are important nursery and feeding grounds for very large number of marine species (Bilgili et al. 2005; Rostamkhani 2015). Due to the increase in development pressure in coastal zones, estuaries have been acting as direct repositories of discharged contaminants and SPM (Bilgili et al. 2005; Silva et al. 2015). Unfortunately, the estuaries are not capable of assimilating SPM indefinitely. Therefore, predicting the transport and fate of pollutants in the estuaries is considered to be a challenging task (James 2002; Gleizona et al. 2003; Lopes et al. 2005; Gisen et al. 2015).

The coastal drainage system of Tanzania, which occupies 20% of the Tanzania land area is drained by several river networks discharging their water to the Indian Ocean (ASCLME 2012). The coastal rivers contribute about 50% of the total surface run off (Francis et al. 2001). Pangani river, with a mean annual discharge of 27 m³/s is the fifth largest river along the coast of Tanzania (ASCLME 2012). The other four largest rivers along the Tanzanian coastal drainage system (Welcomme 1972; Hafslund 1980; Francis et al. 2001) with their mean annual discharges shown in brackets are: the Rufiji (900–1133 m³/s), the Ruvuma (475 m³/s), the Ruvu (63 m³/s) and the Wami (63 m³/s). Estuaries are among the major prominent features located at the mouths of these rivers (ASCLME 2012).

Climate changes and anthropogenic activities related to demand for water for irrigation and hydropower

developments are considered to have significantly reduced the fresh water discharges of the above rivers at least during the last 50–60 years (IUCN 2003; Shaghude 2006; Duvail and Hammerlynck 2007; ASCLME 2012). Apart from the irrigation and hydropower developments, livestock developments and land use changes on the upper catchments of the above rivers have also contributed to the degradation of the river basins, with corresponding reduction in the fresh water discharges of the rivers. In some of the rivers such as the Pangani, Wami and Ruvu, the situation is considered to be critical with multipliable socio-economic conflicts and potential ecological and environmental impacts at the coast (IUCN 2003; Shaghude 2006).

Currently, there is insufficient information on how these estuaries respond to the changes resulting from the rivers upstream anthropogenic activities and climate changes. Particularly, there is a general lack of information on the pattern of transport of the discharged SPM to the estuaries and the Indian Ocean which borders these estuaries. There is also a general lack of information on how the transport and dispersion pattern of the SPM discharged to the estuaries is related to the changing monsoon wind pattern as well as the tidal forcing from the Indian Ocean.

Although hydrodynamic modeling software such as ROMS, MIKE 21 (HD) and MIKE 3 are increasingly becoming commonly in predicting the hydrodynamic conditions of estuaries and bays (Zacharias and Gianni 2008; Webster et al. 2014), their usage in Tanzania is still at an infant stage. Noteworthy applications of ROMS in Tanzania include few studies on the Zanzibar Channel (Mayorga-Adame 2007; Garcia-Reyes et al. 2009) and the recent study conducted along the coast of Tanzania (Mahongo and Shaghude 2014). The applications of MIKE 21 in Tanzania include the study of hydrodynamics in estuaries (Mrema 2012) and determination of pollution dispersion pattern due to anthropogenic activities.

In view of the above presented examples on the usage of ROMS and MIKE 21 software in modeling coastal hydrodynamic processes in Tanzania coastal waters, it is becoming obvious that the availability of hydrodynamic modeling software like ROMS, MIKE 21 (HD) and MIKE 3 in Tanzania has opened a new path of studying hydrodynamics of coastal waters, and estuaries are not exceptions. The present study was therefore formulated with the aim of using MIKE 21 software in studying the hydrodynamic processes of the Pangani estuary and filling the knowledge gaps on how the changing monsoon pattern and tidal forcing influence the transport and dispersion pattern of the SPM discharge. The specific objectives of the study were: (i) to determine the magnitude and direction of tidal currents in the estuary (ii) to identify the weak current zone which in turn enhance the deposition of SPM (iii) to examine the

influence of tidal current on erosion, transport and deposition of SPM in the estuary.

Methodology

Study Area Description

The Pangani River Basin, with an area of about 43,000 km³ is one of the largest River basins along the Tanzania Indian Ocean drainage system (Fig. 1). Geomorphologically, the basin falls under two geomorphologic units, namely, 1- the highlands which rises from 1000–2000 m above sea level, characterized by rich volcanic soils abundant rainfall (1200–2000 mm per year), high biodiversity, intensive cultivation, urbanization and highly populated rural areas, with annual growth rates of >4%, and 2- the lowlands (also known as the “*Maasai steppe*”) consisting of low sloping

terrain, (generally less than 1000 m above sea level) descending to the coastal plain and characterized by relatively low rainfall (<500 mm per year) and low species biodiversity scattered (IUCN 2003). The Pangani Estuary which is located on the downstream part of the Basin is funnel shaped and meso-tidal, where the mean tidal range is about 3.9 meters (Sotthewes 2008). The river mouth of the estuary lies between Zanzibar channel to the South and the Pemba channel to the North. The climate of the entire Pangani coastal area is warm and humid with mean day-time temperature, ranging from 22 °C to 30 °C and an average precipitation rate of 1100 mm/year (UNEP 1998).

The entire coastal of Tanzania is affected by the monsoon winds whose direction changes on seasonal basis and Pangani estuary is not an exception (Mahongo et al. 2012). According to Mahongo et al. (2012), the monsoon winds system, reverses in direction from SE (March to September) to NE (October to March). The former winds are associated with long rains and stronger ocean currents of up to 2 m/s, while the later are associated with short rains and weaker ocean currents (Newell 1959). From June to September or early October the winds are strongest and often stormy and the precipitation rates are minimal (Shaghude 2006; Mahongo et al. 2012). Wind speeds are usually weaker with highest variability in direction between October and December. The wind velocity data from Tanzania Meteorological Agency (TMA) located about 52 km north of the Pangani estuary shows that the wind speeds vary between 1.5 m/s and 8 m/s (average 5 m/s) during the period of the NE monsoon (Mahongo et al. 2012). However, during the SE monsoon season, the winds are generally stronger with an average of 8 m/s (UNEP 1998).

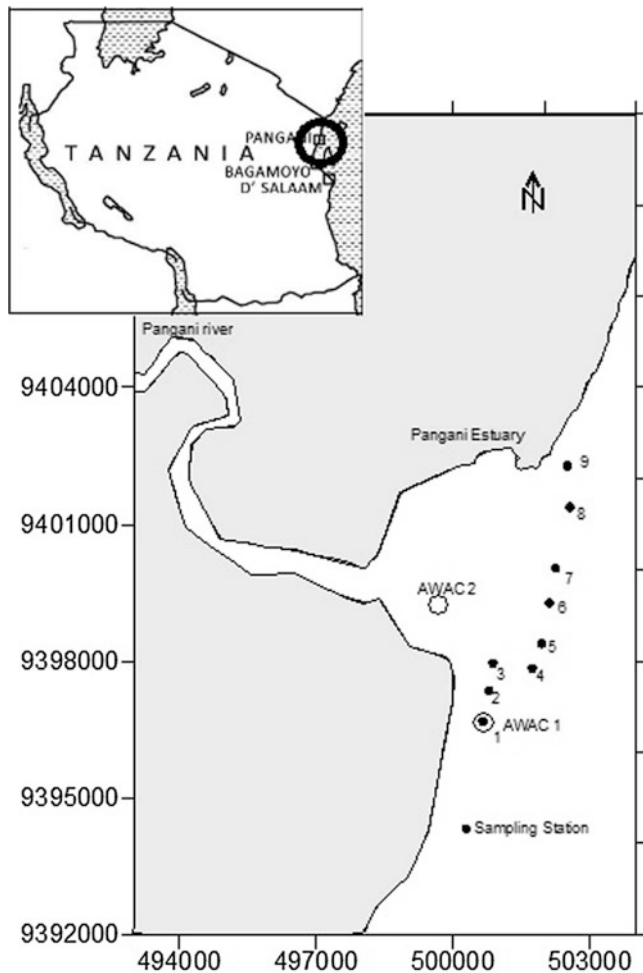


Fig. 1 A map of the Pangani estuary, showing the sampling stations for the SPM fluxes across the river mouth

Sampling and Measurements of SPM Fluxes

Sampling and measurements of SPM fluxes were achieved through deployment of sediment traps for a period of one year, spanning from December 2010 to November 2011. The traps were constructed from local flowerpots and PVC pipes; with the internal diameter of about 100 mm and height of 500 mm, giving the aspect ratio of 1:5. The design of sediment traps were purposely for trapping SPM vertically from the sea surface. The mouth of each trap was placed at least 50 cm from the seafloor to trap vertical flux particles (English et al. 1994; Muzuka et al. 2010). Steel bars were used to fix the traps to the sea floor to avoid displacement by currents and waves. Funnels were placed at the top of each trap to retain the trapped SPM fluxes and to avoid the re-suspension fluxes due to tidal currents and to avoid intrusion by living organisms.

Nine sampling stations were established across the river mouth from South to North (numbered from 1 to 9 in Fig. 1) to enclose the entire river mouth but also to ensure that both the influence of SE and NE monsoons are covered. The selection of sampling stations took into consideration of the impacts of flood-ebb tidal phase variability along the main axis of the river. Sediment traps were retrieved and re-deployed on monthly basis. Retrieved SPM in traps, were carefully poured into the clean containers and then transported to the Institute of Marine Sciences (IMS) laboratory for further quantification and analysis.

In the laboratory, the samples from the sediment traps were transferred into plastic containers and left standing for a period of one week; allowing for fine particles to settle. The water in the container was removed using a syringe, to avoid sediment re-suspension. The water left in the containers, was allowed to evaporate under room temperature conditions. The sediments were finally oven-dried to constant weights at a temperature of 60°C. The dried samples, were weighed and then net sediment fluxes were determined according to English et al. 1994; Muzuka et al. 2010 (Eq. 1).

$$F = \frac{W_s - W_e}{A_{st} \times t} \quad (1)$$

Where: F = sediment flux; W_s = the weight of container with sediment; W_e = the weight of the empty container; A_{st} = Cross-section area of the sediment trap; t = time duration between sediments traps deployment and retrieval.

Measurements of SPM Concentration

Water samples for determination of SPM concentration were collected at 9 sampling stations along the longitudinal axis of the estuary (Fig. 1). The sampling was conducted between January and June, 2011 to encompass both dry and rain seasons. The samples were stored in plastic bottles and transported to the Institute of Marine Sciences Laboratory for further analysis. The SPM concentration in mg/l was determined gravimetrically following the procedures outlined by Strickland and Parsons (1972). Water samples were filtered through pre-weighed 0.45 μm GF/F filter. Thereafter, the filters were rinsed with distilled water to remove salts and then dried to constant weight.

Measurements of Waves and Tidal Currents Velocities

Measurements of waves and tidal currents velocities were determine using a self-recording Acoustic Wave and Current

(AWAC) profiler between December 2010 and April 2011. The profiler had a pressure sensor used to measure the tidal elevations. The AWAC was moored at two locations (station 1 and 2; Fig. 1). The AWAC was positioned at about 8 m water depth and the sensors were kept at an elevation of about 0.5 m above the seabed. The profiler was programmed to record the current velocity profiles after every 10 min. while the vertical current velocity profiles were recorded at 2 m intervals from the top of the sensor to the sea surface. The wave data was recorded at 1 hour intervals.

Hydrodynamic Model Set-Up

Hydrodynamic model was carried out using MIKE 21; where the bottom shear stress, wind shear stress, barometric pressure gradients, Coriolis force, momentum dispersion, evaporation, flooding and wetting were considered as forcing functions. For the purpose of model set up, the model domain was divided into several smaller model domains of velocity and momentum. The vertical velocity domain was calculated using continuity Eq. (2). Horizontal momentum in both x and y direction were calculated using momentum Eqs. (3) and (4), respectively. These Eqs. (2, 3, and 4) were integrated in the vertical direction to describe the flow and water level variation as described by Zacharias and Gianni (2008). For numerical stability, the model used an alternate direction implicit scheme in accordance with Duarte (2008).

$$\frac{\partial \xi}{\partial t} + \frac{\partial p}{\partial x} + \frac{\partial q}{\partial y} = 0 \quad (2)$$

$$\begin{aligned} \frac{\partial p}{\partial t} + \frac{\partial}{\partial x} \left(\frac{p^2}{h} \right) + \partial \left(\frac{pq}{h} \right) + gh \frac{\partial \xi}{\partial x} + \frac{gp\sqrt{p^2 + g^2}}{c^2 h^2} \\ - \frac{1}{\rho_w} \left[\frac{\partial}{\partial x} (h\tau_{xx}) + \frac{\partial}{\partial y} (h\tau_{xy}) \right] - \Omega q - fVV_x \\ + \frac{h}{\rho_w} \frac{\partial}{\partial x} (pa) = 0 \end{aligned} \quad (3)$$

$$\begin{aligned} \frac{\partial p}{\partial t} + \frac{\partial}{\partial y} \left(\frac{q^2}{h} \right) + \partial \left(\frac{pq}{h} \right) + gh \frac{\partial \xi}{\partial x} + \frac{gq\sqrt{p^2 + g^2}}{c^2 h^2} \\ - \frac{1}{\rho_w} \left[\frac{\partial}{\partial y} (h\tau) + \frac{\partial}{\partial y} (h\tau_{xy}) \right] - \Omega q - fVV_y \\ + \frac{h}{\rho_w} \frac{\partial}{\partial y} (pa) = 0 \end{aligned} \quad (4)$$

Where: τ_{xx} , τ_{xy} , τ_{yy} are components of effective shear stress; V , V_x , V_y are wind speed and components in x and y direction (m/s); Ω (x,y) is a Coriolis force, latitude dependent (m); ρ_a is atmospheric pressure ($\text{kg m}^{-1} \text{s}^{-1}$) is a

density of water (kg/m^3); $f(V)$ is a wind friction factor, C is Chezy resistance ($\text{m}^{1/2}/\text{s}$); g is acceleration due to gravity (m^2/s); t is time (s); p, q is flux densities in x and y direction ($\text{m}^3/\text{s}/\text{m}$); h is water depth (m), ζ is a surface elevation (m). The effective shear stress ($\tau_{xx}, \tau_{xy}, \tau_{yy}$) in the momentum equations contains fluxes due to turbulence, vertical integration and sub-grid scale fluctuations. The formulation of the eddy viscosity in the equations was implemented based on the velocity as described in Eq. (5).

$$\text{Eddy viscosity} = \frac{\partial}{\partial x} \left\{ h.E \frac{\partial u}{\partial x} \right\} + \frac{\partial}{\partial y} \left\{ h.E \frac{\partial u}{\partial y} \right\} \quad (5)$$

Where u is the velocity (m/s) in the x - direction and h is the water depth (m) and E is the eddy viscosity coefficient. The eddy viscosity coefficient was specified using a time varying function of the local gradient in a velocity. The eddy viscosity coefficient (E) was calculated using Eq. (6) that puts into consideration of the Smagorinsky (1963) concept.

$$E = c_s^2 \Delta^2 \sqrt{\left(\frac{\partial u}{\partial x} \right)^2 + \frac{1}{2} \left(\frac{\partial u}{\partial y} + \frac{\partial v}{\partial x} \right) + \frac{\partial v}{\partial y}} \quad (6)$$

Where u, v are depth-averaged velocity components in the x and y -direction Δ is the grid spacing and c_s is a constant chosen in the interval of 0.25 to 1.0. The driving force due to wind was calculated from the following quadratic Eq. (7):

$$C_w \frac{\rho_{\text{air}}}{\rho_{\text{water}}} W^2 \quad (7)$$

Where: C_w is the wind friction coefficient ρ is the density and W is the wind velocity above the sea surface. Normally a wind friction coefficient of 0.0026 provides good results for moderate and strong wind in the open sea. For weak winds, however smaller coefficients can be used (Zacharias and Gianni 2008).

The bed resistance was estimated using Chezy number which is also a function of Manning number. The Chezy number and Manning number were estimated using Eqs. (8 and 9):

$$\text{Manning Number} = \frac{g \cdot u \cdot |u|}{C^2} \quad (8)$$

Where g is the acceleration due to gravity, u is velocity and C is the Chezy number. The manning number was converted to Chezy number using Eq. 9.

$$C = m \cdot h^{1/6} \quad (9)$$

Where, m is the manning number. The units of Chezy (C) and Manning numbers (m) are $\text{m}^{1/2}/\text{s}$ and $\text{m}^{1/3}/\text{s}$, respectively.

Table 1 Summary of parameters (and their values) used for the model set up.

Parameters	Values
Initial water level	0.23 m
Time steps	100 sec.
Number of Time steps	4500
Flood and ebb	Ebbing depth 0.2 m , Flooding depth 0.3 m
Wind friction coefficient	0.0026
Eddy viscosity	Smagorinsky formulation velocity based constant 0.5
Bed resistance	Manning number coefficient 32

Model Dataset

Water level, wind speed and direction and tidal currents were considered in the model simulation. These dataset were collected during the field campaigns conducted between December 2010 and August 2011. Data on wind speed and direction were obtained from the Tanzania Meteorological Agency (TMA) at Tanga station; the closest meteorological station is approximate 50 km to Pangani estuary. The water levels were recorded at each end of the open boundary; established in South, North, West and East of the estuary. The bathymetry setting of the model was accomplished by importing the navigational chart data, supplemented with echo soundings field measurements. During the echo-sounding survey, spot depth measurements were collected simultaneously with their corresponding geographic locations; recorded using a hand-held GPS. Processing of the bathymetric data included tidal corrections, followed by inspection of the actual bathymetric data. The true depths (corrected depths) were ranged from 1.5 to 20m. The data covered both upstream and downstream parts of the estuary described by the width of 20000 m and the length of 16000 m to ensure a uniform flow pattern at the model boundaries. Other parameters used for model set up are summarised in Table 1.

Model Calibration

The simulated tidal currents and water elevation in each open boundary were extracted and compared with their corresponding measured data. The model calibration in the present study involved three variables: bed coefficient, coefficient of eddy viscosity and the coefficient of wind friction. The variables were regulated to ensure that the simulated data agreed with the measured data. The eddy viscosity was regulated by selecting various values from a set of in built generated values, starting with a default value of $0.5 \text{ m}^2/\text{s}$. As the eddy viscosity approached $1.2 \text{ m}^2/\text{s}$, the simulated

data showed a good agreement with the measured data. The bed coefficient was estimated using Manning numbers, which were assigned values ranging between $20 \text{ m}^{1/3}/\text{s}$ and $40 \text{ m}^{1/3}/\text{s}$ (The range recommended by DHI 2007). The wind friction coefficient was included in the model calibration as a constant value of 0.0026. The correlation between the simulated and the measured data was tested by linear regression analysis while their amplitude adjustment (Eq. 10) was quantified by the Root Mean Square (RMS).

$$\text{RMS} = \left\{ \frac{1}{N} \sum_{i=1}^N [\zeta_{\text{obs}}(t_i) - \zeta_{\text{model}}(t_i)]^2 \right\}^{1/2} \quad (10)$$

$\zeta_{\text{obs}}(t)$ and $\zeta_{\text{model}}(t)$ are the observed and the modeled current velocity, N is the number of time series.

Results

Temporal and Spatial Variation of SPM Fluxes

The deposition of SPM preferentially occurred on either side (North or South) of the longitudinal axis of the river (Figs. 2, 3, 4, 5, 6, and 7), with minimum deposition observed at the middle parts of the river mouth, particularly at stations 4, 5, 6 and 7 (Figs. 2, 3, 4 and 5). The deposition of SPM increased on either side of the river mouth; forming a parabolic curve pattern with a maximum values occurring at a distance of about 3.3 km North /South of the central axis (Fig. 2). The observed pattern of SPM fluxes and its deposition from December 2010 to August 2011 revealed that in December 2010, the SPM fluxes were minimum ($66 \text{ gm}^{-2}\text{d}^{-1}$) at the central part of the river mouth and increasing gradually with distance from the central axis on either side of the river mouth with a slight bias to the northern side ($R^2 = 0.79$, at confidence interval of 95%). The maximum SPM fluxes observed

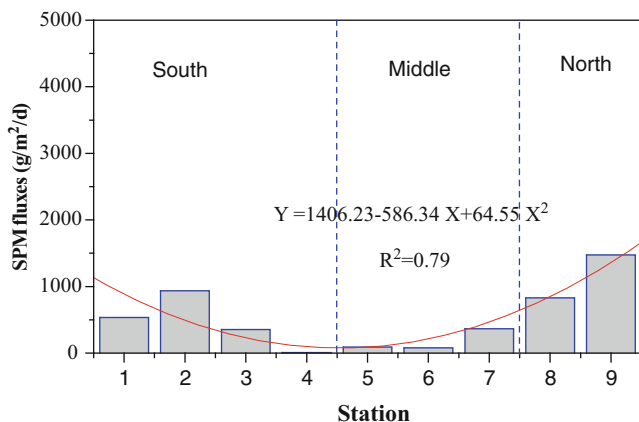


Fig. 2 Spatial variation of SPM fluxes observed in December 2010

in December was approximately $1500 \text{ gm}^{-2}\text{d}^{-1}$ which occurred at station 9. In January 2011, the SPM fluxes resembled the pattern observed in December ($R^2 = 0.83$), but with the fluxes reduced from two to four times the fluxes observed in December (Fig. 3).

In February 2011, the SPM fluxes maintained the parabolic pattern ($R^2 = 0.82$) shown during the previous months but with a stronger bias towards the south (Fig. 4). The highest deposition of SPM fluxes ($1800 \text{ gm}^{-2}\text{d}^{-1}$) were observed at station 2 located on the southern side of the river mouth and then decreased southward from station 2 to 9. Similarly in April 2011, the SPM fluxes maintained the parabolic pattern ($R^2 = 0.77$) shown by the previous months but with lower particles settling over most of the stations proximal to the main axis of the river mouth (Stations 3, 4,5,6,7 and 8) (Fig. 5). In June 2011, the SPM fluxes maintain the parabolic curve ($R^2 = 0.55$), with an almost symmetrical pattern about the central axis (Fig. 6). Some particles settled at the station located proximal to the middle of the river mouth (Stations 5 and 6); creating a central peak in addition to the other two peaks (Fig. 7). The site of highest deposition shifted from south in February to north in August. However the amount of

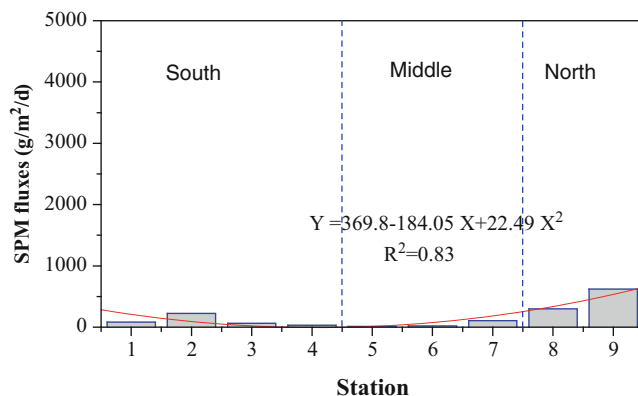


Fig. 3 Spatial variation of SPM fluxes observed on January 2011

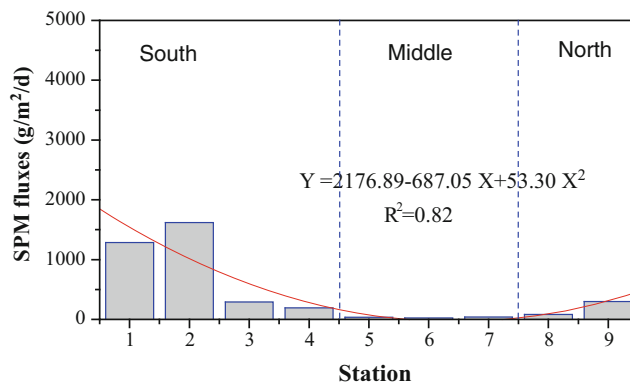


Fig. 4 Spatial variation of SPM fluxes observed on February 2011

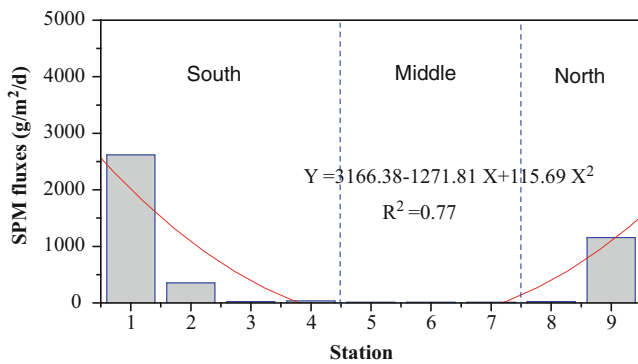


Fig. 5 Spatial variation of SPM fluxes observed on April 2011

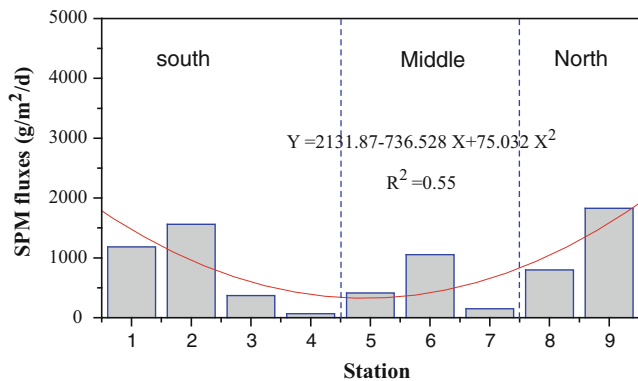


Fig. 6 Spatial variation of SPM fluxes observed on June 2011

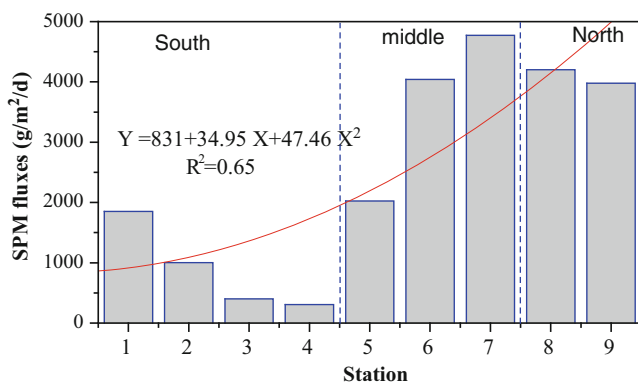


Fig. 7 Spatial variation of SPM fluxes observed on August 2011

SPM deposited in the northern part was relatively higher than in the southern part.

Comparison of Spatial Variation of SPM Between SE and NE Monsoon Wind

The SPM fluxes on the sampling stations (1–9) were compared between the NE and SE monsoon seasons (Fig. 8). In

both sides of the estuary (northern and southern), the SPM fluxes were higher during the SE monsoon season compared to the NE monsoon season. The SPM fluxes on the southern parts of the estuary (Station 3 and 4) did not show major variations between the two seasons. Station 6, 7, 8 and 9, (located in the north of the estuary) received extremely SPM fluxes during the SE monsoon season than during the NE monsoon season (Fig. 8).

Tides and Waves and Mean Currents on the Pangani Estuary

Analyses of the tidal currents data revealed that tides are semi-diurnal with maximum spring tidal range of about 3.5 m and maximum neap tidal range of about 3.0 m. Analyses of the pattern of the mean current direction is summarized in Rose diagrams (Fig. 9). The results show that the mean currents on the River mouth changed with season. During January to March (representing the NE monsoon season) the mean currents flowed southwards (Fig. 9). During April (representing the SE monsoon season) the mean currents flowed northwards (Fig. 9). Moreover the mean currents during February and March were more variable (with relatively more components) than during January and April.

The monsoon induced waves in the Pangani estuary recorded from January to March are presented in Fig. 10. From January to nearly the end of February and from the 7th to 11th March, the wave heights were relatively high (>1.6m). From the end of February to 6th March the wave heights were relatively low (0.4 to 1.4m). The wave direction from January to April represented in Rose diagram, indicate that the main direction of waves was consistently southeasterly (Fig. 11). Analysis of the data on wave spectra (involving the direction and the frequency of waves) from January to April, 2011 revealed significant monthly variations (Fig. 12). In January the highest frequency of the wave occurred between 100° to 150° while in February there were two peaks, all centered between 100° and 150° (Fig. 12). The first peak was located at 0.1Hz while the second was located at about 0.3 Hz. In March there were two prominent peaks both located at 0.13Hz but in different directions (100° and 270°). In April the wave spectrum was characterized by two prominent peaks, the first one was highly variable in direction (0–360°) but centred at 0.1 Hz (Fig. 12). The second peak was centred at 0.3 Hz with a general direction of 100°.

River Discharge and SPM Concentration

The results of river discharge and SPM concentration are presented in Fig. 13. The results showed that minimum river

Fig. 8 Comparison of spatial variation of SPM fluxes during SE and NE monsoon

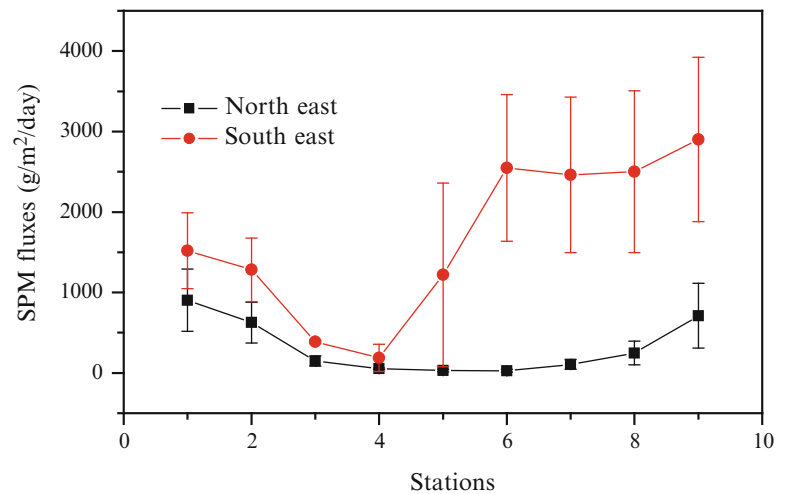
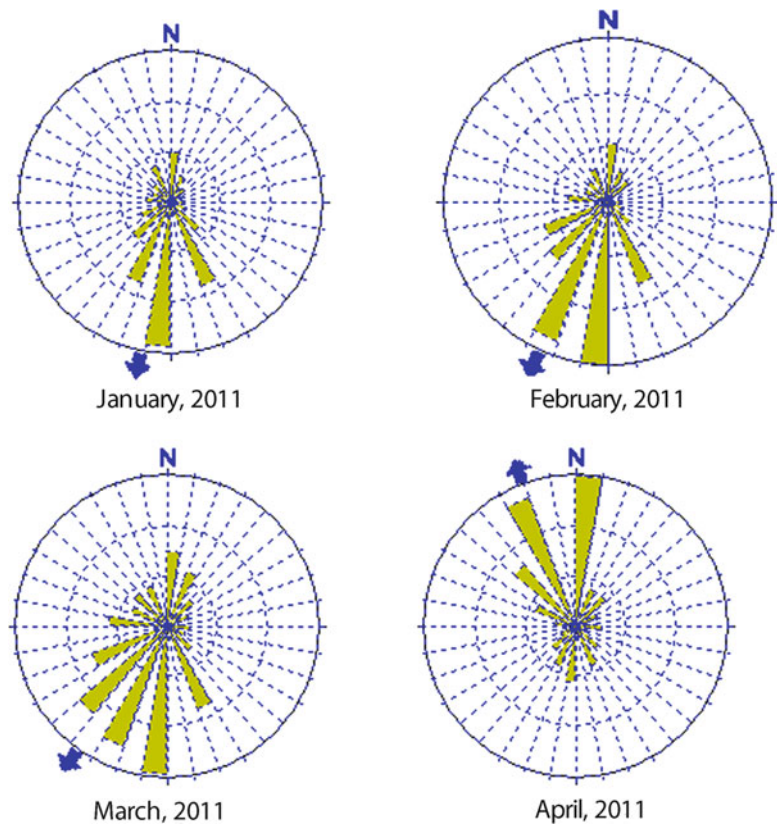


Fig. 9 Rose diagrams showing the direction of Currents from January to April 2011



discharge occurred between December and February ($20 \text{ m}^3/\text{s}$) while maximum discharge ($97 \text{ m}^3/\text{s}$) occurred in May (Fig. 13a). The SPM concentration in the estuary showed similar trends with that of river discharge data (Fig. 13b). The correlation between the river discharge and SPM concentration showed positive correlation relationship with $R^2 = 0.75$ at a confidence interval of 95% (Fig. 13c). The SPM was negatively correlated with time especially during April to December ($R^2 = 0.85$; Fig. 13d).

Hydrodynamic Model

Simulated and Measured Tidal Currents

The linear regression between predicted and observed currents for both boundaries (upstream and downstream boundaries of the estuary) showed strong positive correlation; where R^2 for the calibrated data were 0.91 and 0.92, respectively (Figs. 14 and 15). The RMS was generally low and satisfactory in both boundaries, ranging from 0.003 to 0.006.

Fig. 10 Time series of wave height in the Pangani estuary: February–March 2011

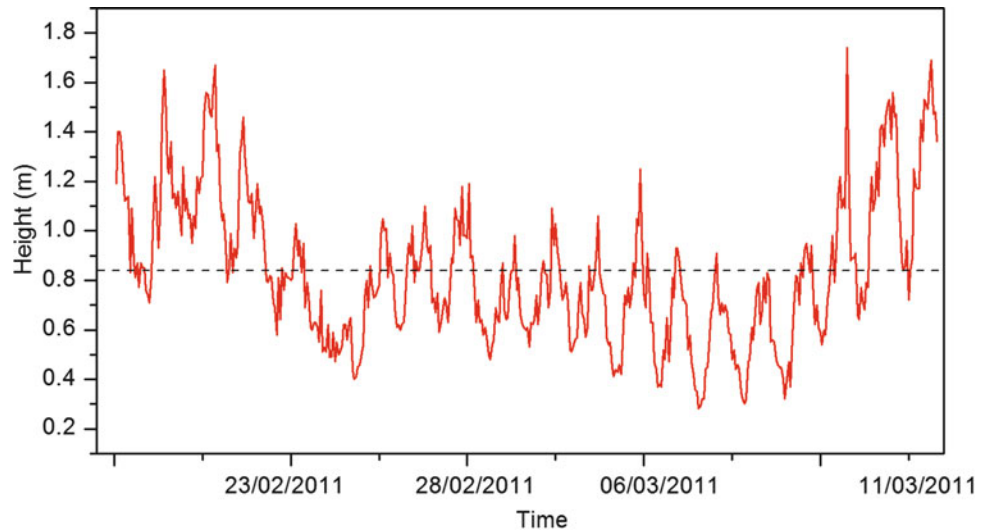
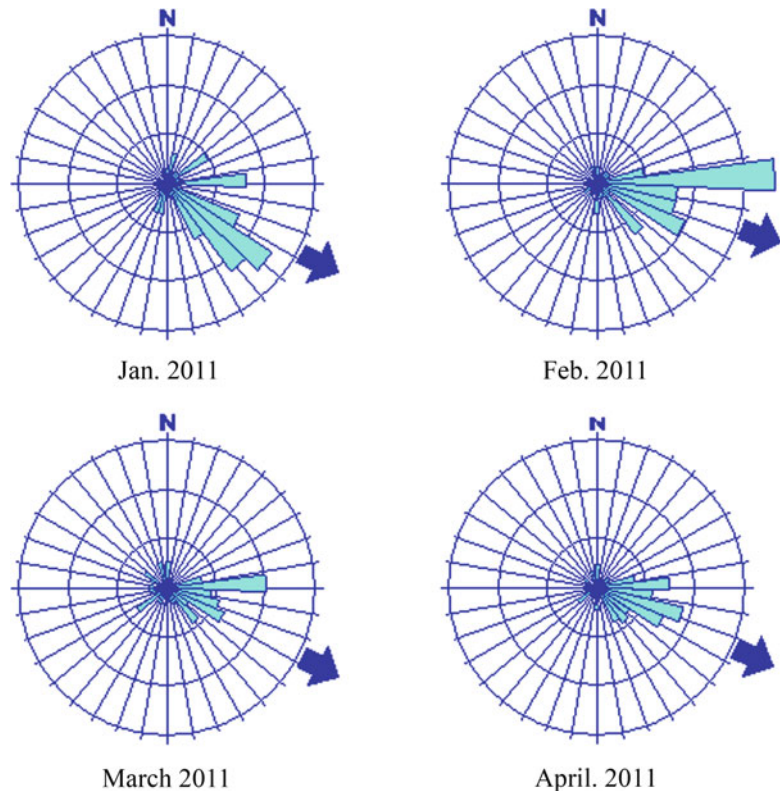


Fig. 11 The main wave direction recorded from January to April 2011



Simulation of the Tidal Currents in the Pangani Estuary

Initially the model simulation results showed relatively sluggish tidal currents (0–0.05 m/s) within the entire estuary (with the exception of areas located further offshore and further upstream parts of the river mouth) where the currents were relatively stronger; greater than 0.05 m/s. During the ebb tidal phase, the ebb currents from upstream side of the river mouth flowed seaward. However as they approached the river mouth, the ebb currents flowed

radially, eastwards, northward and southwards up to at least the first two hours (Fig. 16a, b). During the third and fourth hour, the ebb currents became well established and became relatively stronger than during the first two hours. During this time span, highest intensification of ebb currents were observed along the coastal section on the northern parts of the river mouth. The maximum ebb currents occurred in the middle parts of the estuary, but further offshore and further upstream (towards the inner part of the estuary), the ebb currents became relatively weaker (Fig. 17a, b).

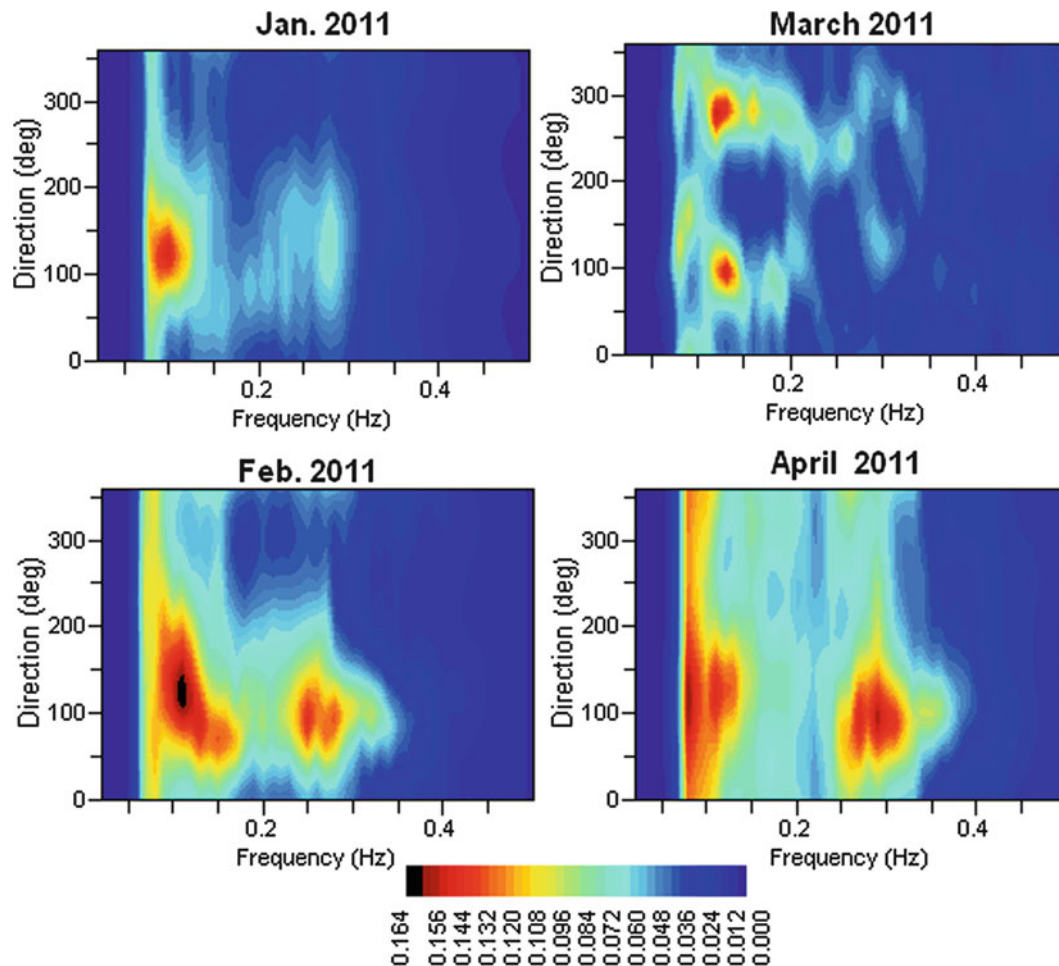


Fig. 12 Wave Spectrum from January to April showing the direction and frequencies

During the 5th and 6th hour of the model simulation, highest ebb currents were observed on the entire width of the river mouth, followed by relatively weaker currents further inshore and further offshore. During this time, a patch of flood tidal currents originating from the southern part of the river mouth, flowing northward were observed (Fig. 18a, b). The flood tidal currents became well established (particularly near the river mouth), during the 7th and 8th hour of the model simulation. The observed pattern of flood tidal currents suggest that the flooding tidal phase first starts on the southern part of the river mouth before it starts on the northern part of the river mouth (Fig. 19a, b). The highly intensified northward flood currents seemed to be more intensive on the northern parts (adjacent to the Pangani Town) than on the southern parts of the estuary opening (adjacent to Bweni village) (Fig. 19a, b). During the 9th and 10th hours, the flood currents were still highly intensified on the river mouth; flowing northward but became more sluggish on the outer parts of the estuary (Fig 20a). By the end of the 10th hour, the flood tidal currents became more intensified on the southern half

of the river mouth compared to the northern half of the river mouth (Fig. 20b).

During the last two hours (11th and 12th) of the model simulation, the strong flood currents on the river mouth became extended further southwards and the northward flowing currents on the outer parts of the estuary were dominated by sluggish currents. Towards the last hour, the northward flowing currents were relatively stronger on the near shore parts of the estuary (with the exception of the estuarine mouth) and sluggish tidal currents were observed further offshore and on the inner parts of the estuary (Figs 21a, b.)

Variation of SPM Fluxes during the Northeast Mooson Season

The SPM fluxes within the Pangani estuary was determined during the NE monsoon season (January and April). The results indicated that, SPM fluxes were relatively higher in

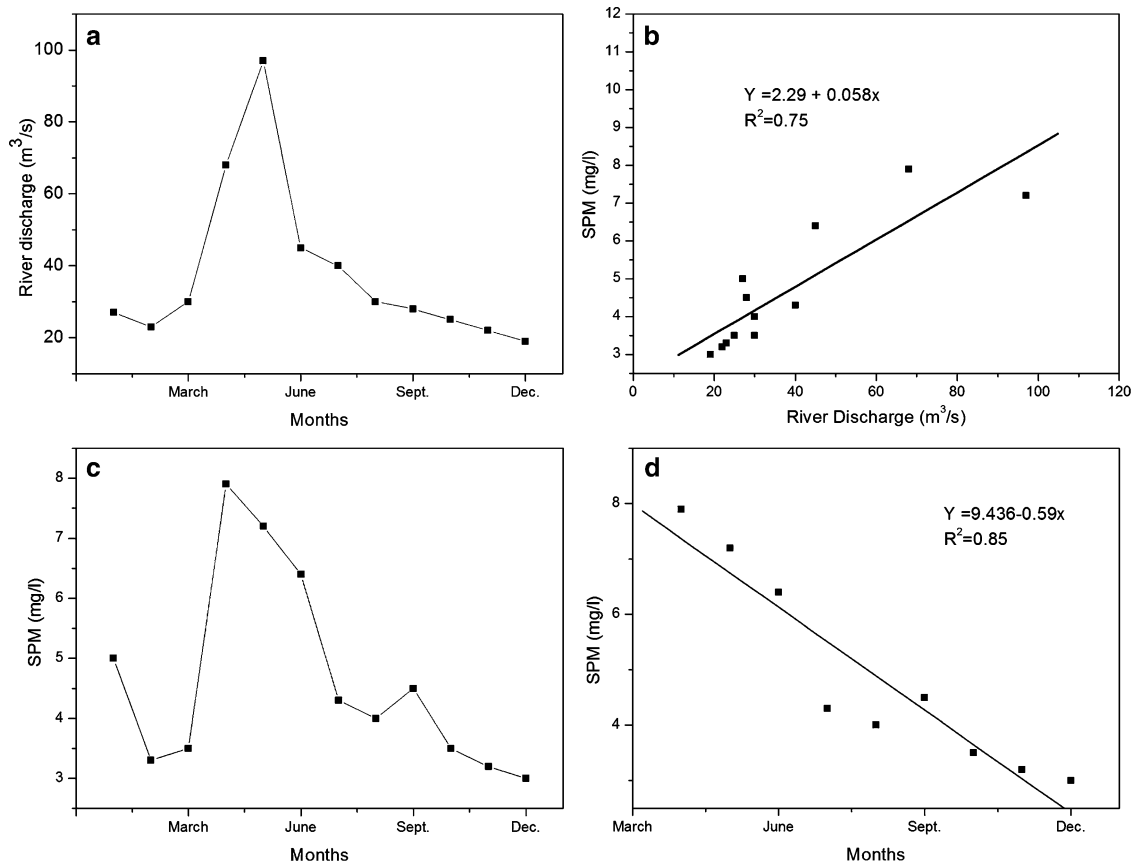


Fig. 13 (a) Monthly discharge of Pangani River (b) Correlation between River discharge and SPM concentration (c) Monthly SPM concentration (d) Correlation of SPM concentration as decreased from April to December

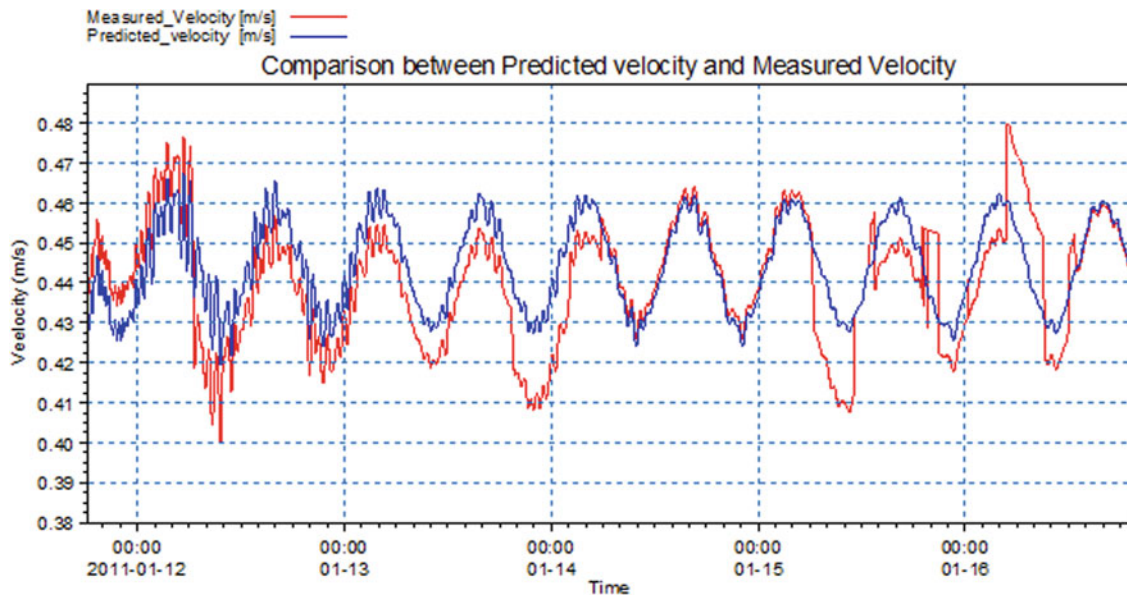


Fig. 14 Computed and Measured Current velocity in upstream after calibration procedures

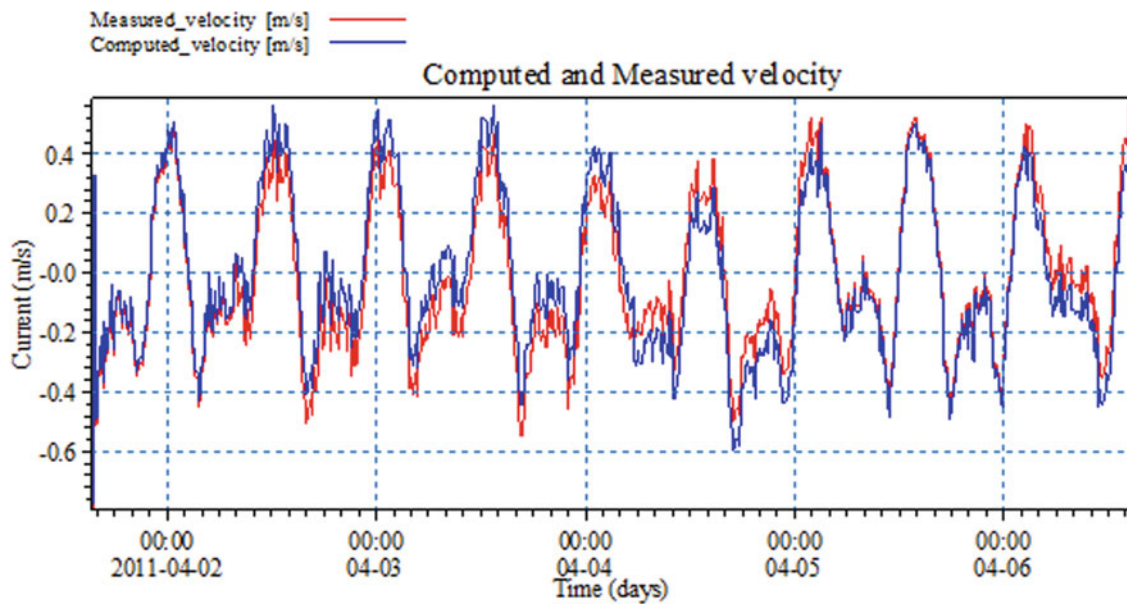


Fig. 15 Computed and Measured Current velocity in downstream after calibration procedures

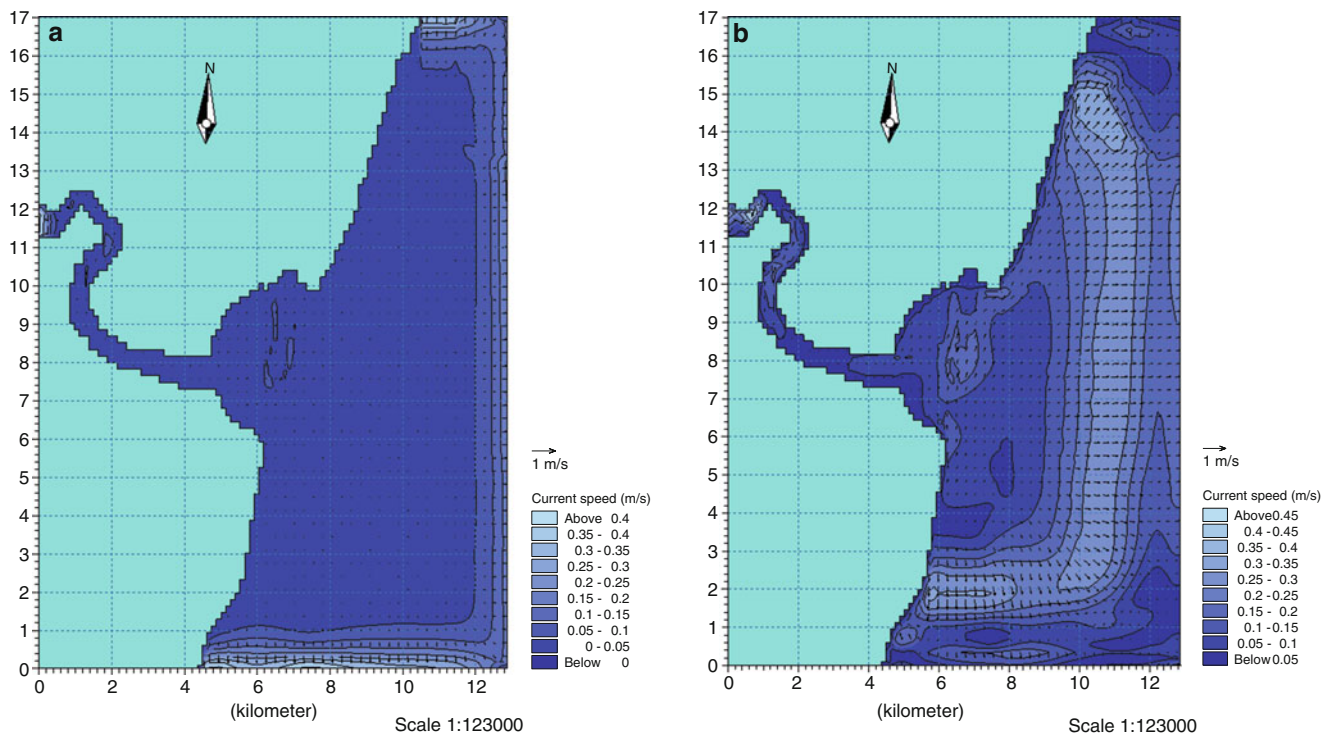


Fig. 16 The simulation of ebb currents in the Pangani estuary (a) After 1 h (b) After 2 h

April than January (Fig. 22a, b). Deposition of SPM on the estuary varied from one trap to another with preferential deposition on the northern parts of the estuary. The SPM fluxes in January and April ranged from 50 g/m²/d to 1804 g/

m²/d, with a peak at the river mouth, however during April the peak extended further northward. During both periods (January and April), the deposition of SPM, indicate that the main direction of SPM transport was northward (Fig. 22).

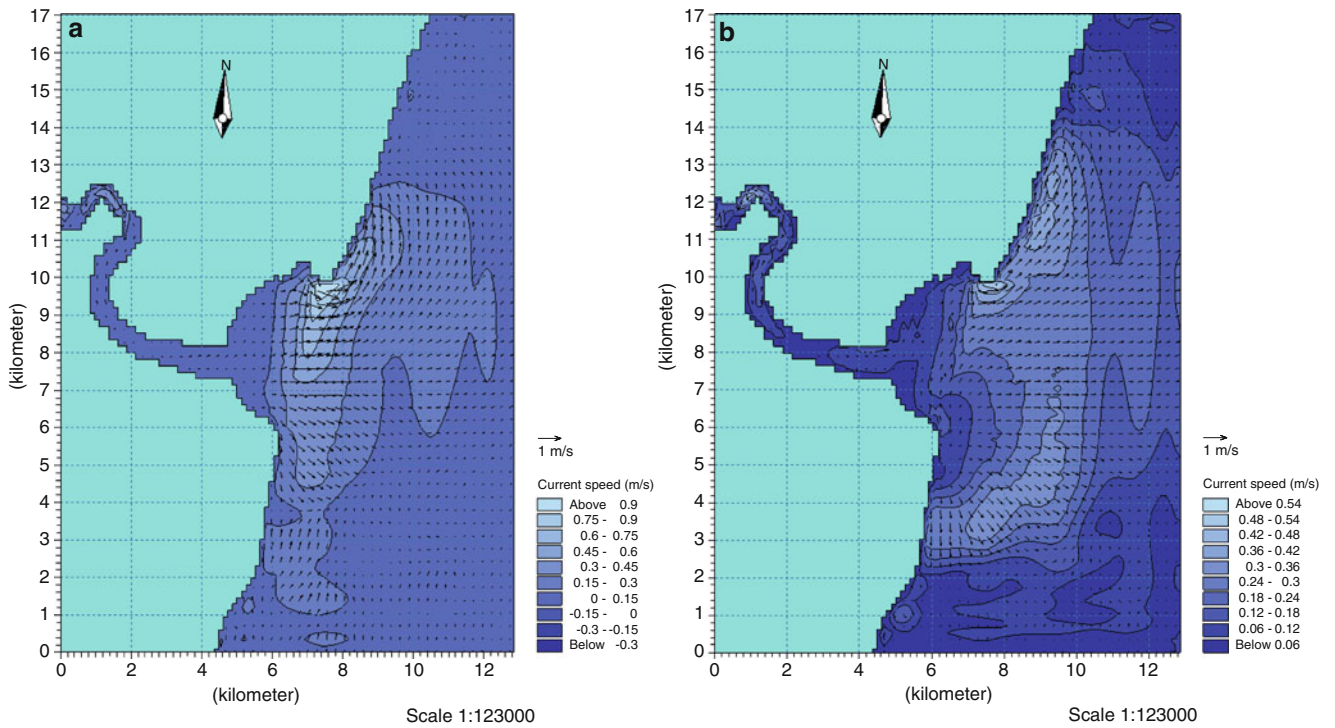


Fig. 17 The simulation of ebb currents in the Pangani estuary (a) After 3 h (b) After 4 h

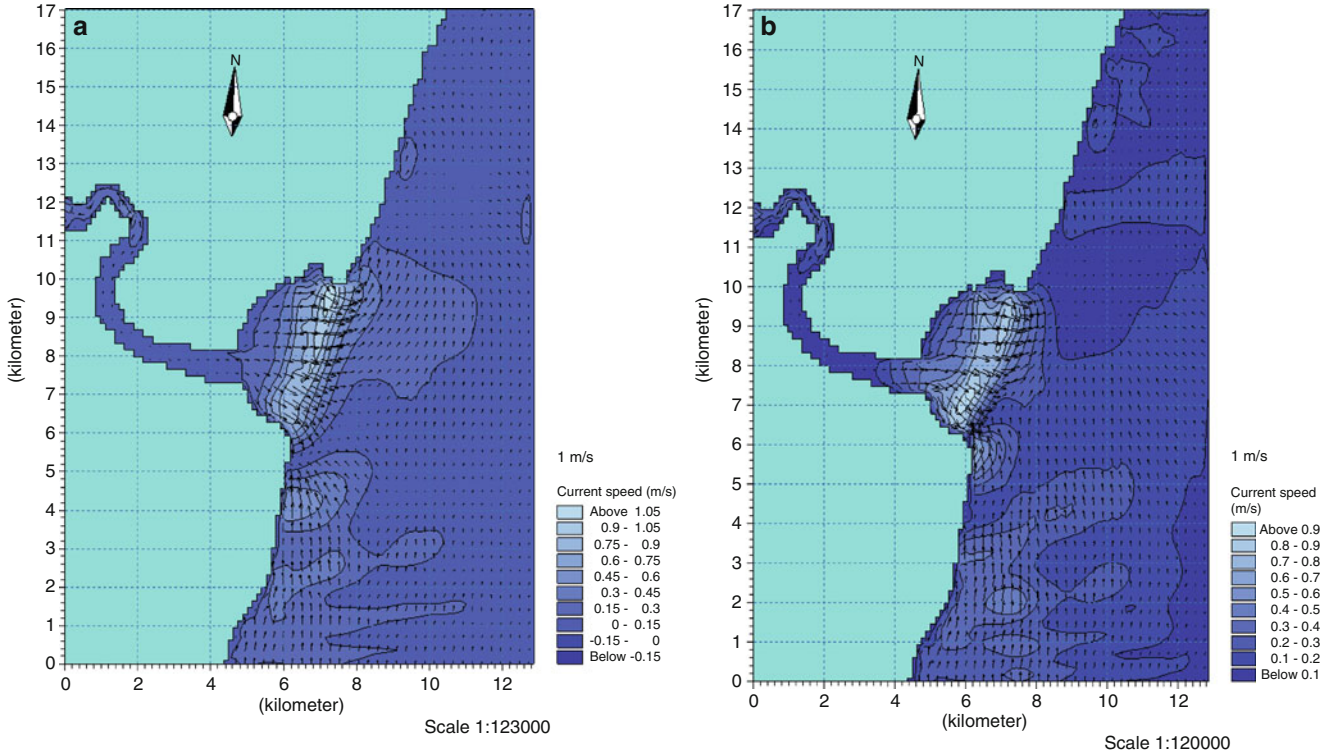


Fig. 18 The simulation of ebb currents in the Pangani estuary (a) After 5 h (b) After 6 h

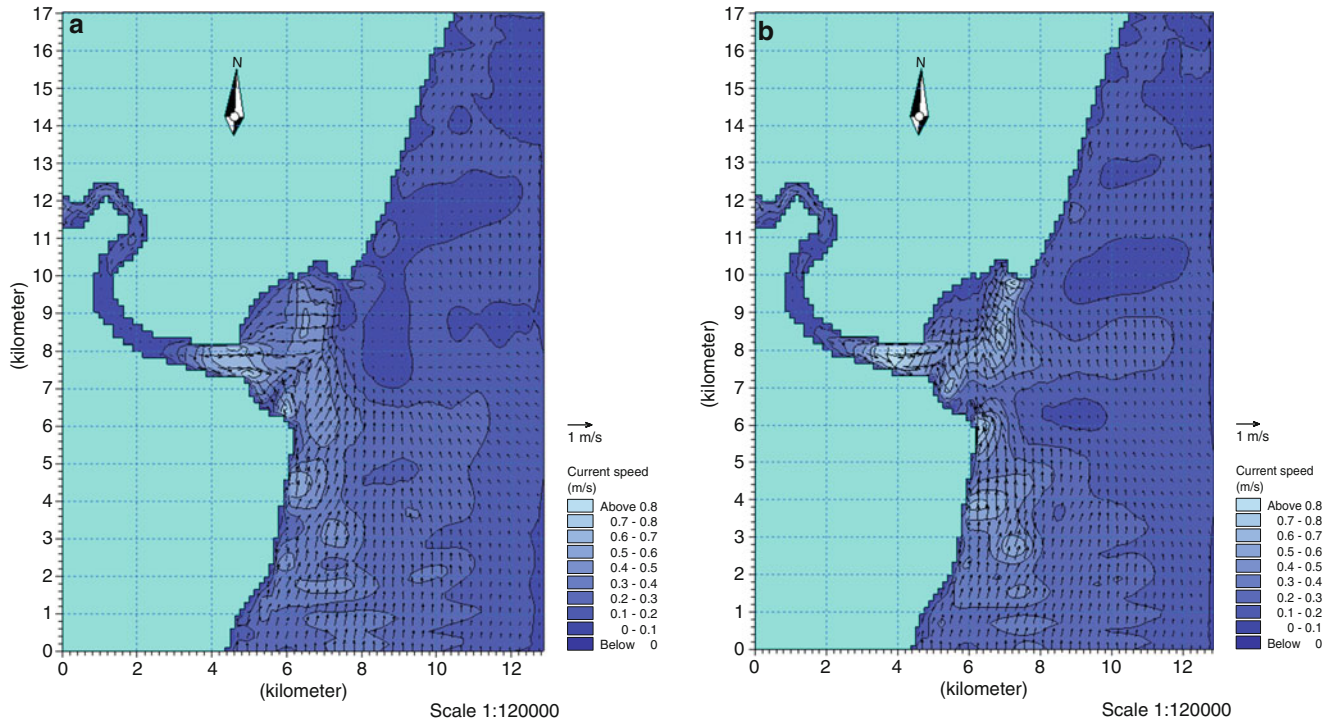


Fig. 19 The simulation of flood currents in the Pangani estuary (a) After 7 h (b) After 8 h

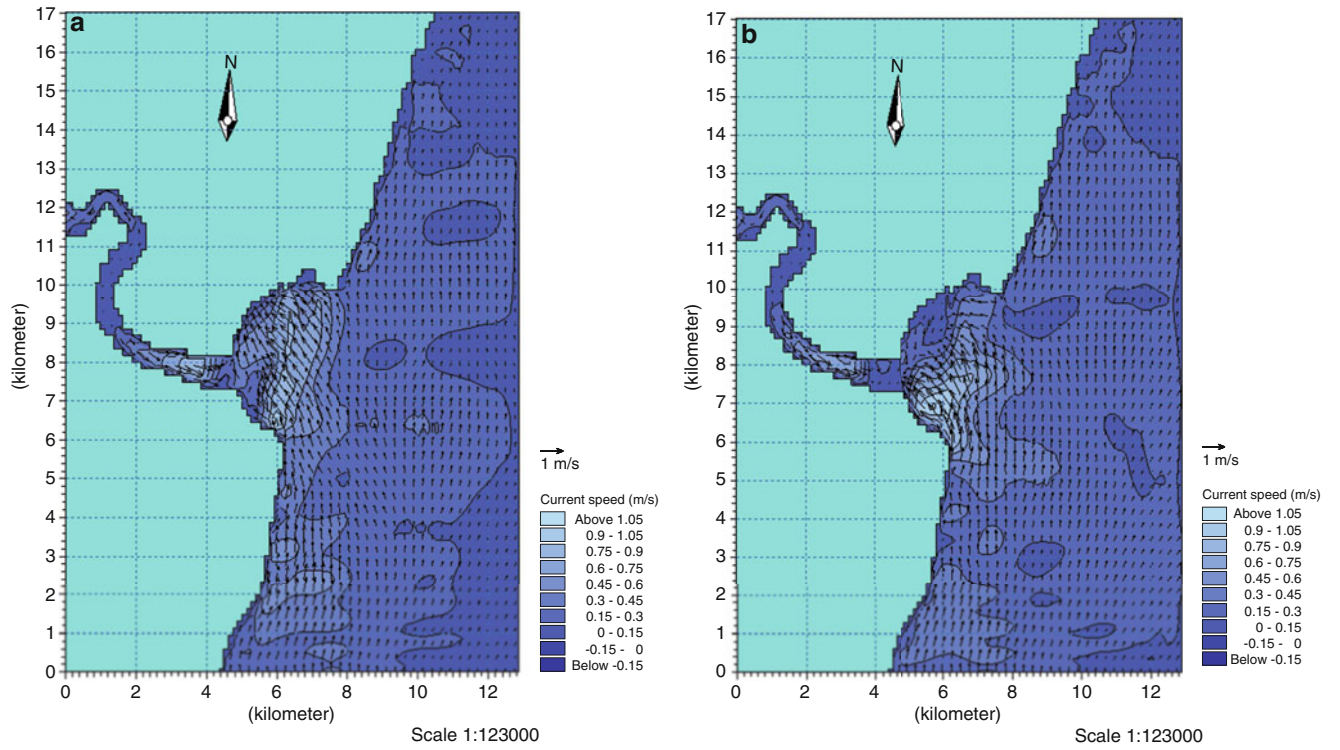


Fig. 20 The simulation of flood currents in the Pangani estuary (a) After 9 h (b) After 10 h

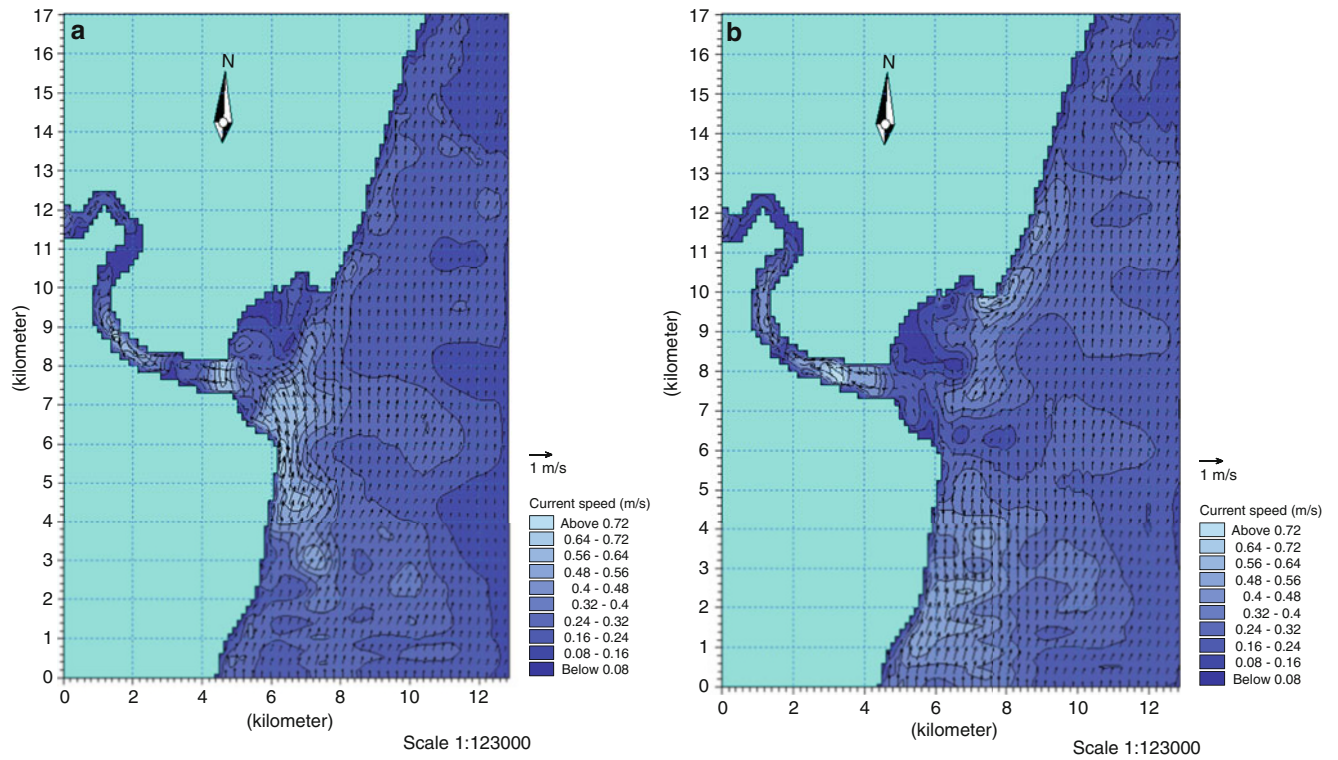


Fig. 21 The simulation of flood currents in the Pangani estuary (a) After 11 h (b) After 12 h

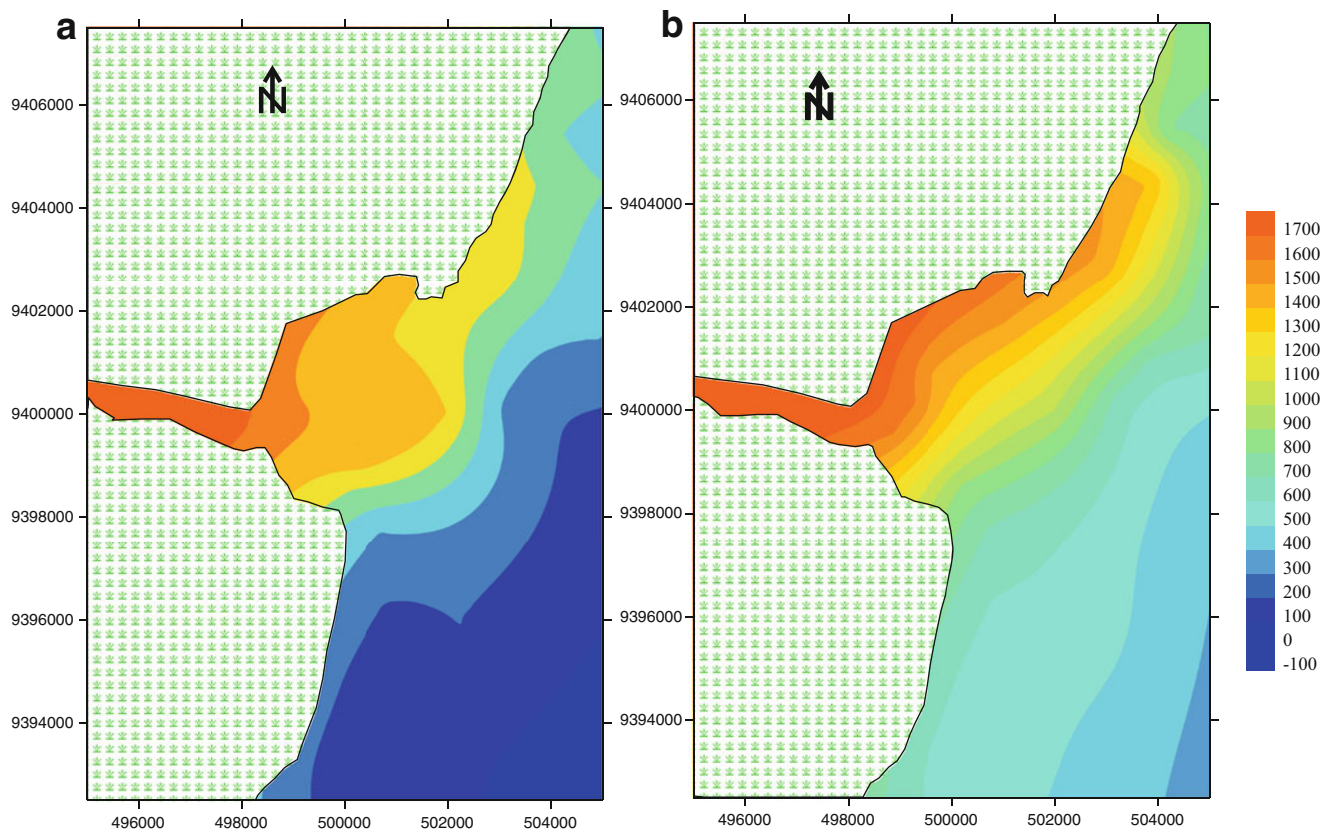


Fig. 22 Contour maps showing the SPM deposition inferred from the sediment traps collections during (a) January and (b) April

Discussion

Spatial and Temporal Variation of SPM Fluxes in the Pangani Estuary

The results presented in Figs. 2, 3, 4, 5, 6, and 7 revealed that the deposition of SPM increased gradually on either side of the River mouth forming a parabolic curve pattern with a minimum value at the middle of the River mouth. The observed pattern has not been reported elsewhere in Tanzania. The observed pattern of SPM fluxes could be attributed to several factors including, change of currents direction in response to monsoon winds and variation in Pangani River flow discharges. The presented results on SPM fluxes on the Pangani Estuary are consistent with other studies conducted along the coast of Tanzania, which show that, sediments transport along the coast are influenced by the seasonal monsoon wind pattern (Muzuka and Shaghude 2000; Shaghude et al. 2003; Mahongo et al. 2012). The observed high SPM fluxes in the southern part of the river mouth during the NE were attributed to the fact that during the NE monsoon season sediments are preferentially transported southward. In response of the changing wind pattern from NE to SE, the SPM fluxes also shifted to the northern parts of the river mouth during the SE monsoon season. In the middle part of the estuary, the SPM deposition were relatively low and this was attributed to the strong tidal and river flow currents which is maximum in the middle parts of the River mouth. The current speed observed on the middle part of the river mouth was as high as 0.5 m/s during ebb phases. The currents of this magnitude are strong enough to prohibit the deposition of fine grained particles in estuaries and coastal water (Liu et al. 2009; Muzuka et al. 2010; Silva et al. 2015).

SPM fluxes were relatively higher on the northern part of the river mouth than on the southern part. This is because SE monsoon winds are relatively stronger compared to the NE monsoon winds (UNEP 1998; Mahongo et al. 2012). Similar Pattern of deposition of SPM have been reported in the southern North sea and Mandovi estuary (India) where the influences of maximum turbidity shifted from one part of the estuary to another depending on the seasonality pattern of the winds. According to Bailey et al. (2011); the SPM concentration changes with direction of winds; increasing in the direction of winds and decreasing in opposite direction of the winds.

River Discharge and SPM Concentration

The variation of Pangani River discharge observed for the whole period of this study is related to the seasonal pattern of rainfall variability. Pangani River Basin is characterized by a

bi-modal rainfall regime with short rain period from October to December (with a peak in November) and long rain season spanning from March to May with peak in April (Kabanda and Jurry 1999; Zorita and Tilya 2002; Kijazi and Reason 2009; Mahongo and Shaghude 2014). The Pangani river discharge data shows that the peak river discharges occur in May. The observed time lag between the precipitations tend to be infiltrated through the thick vegetation cover on the mountains before they could be drained to the Pangani River. According to Kabanda and Jurry (1999) and McSweeney et al. (1998), it is predicted that precipitations on the Pangani River Basin will decrease under the influence of the global climate change, which will in turn affect the River sediment delivery to the beach. This could lead to starvation of the beach in terms of sediment supply, thus resulting into enhanced shoreline erosion.

Hydrodynamic Regime of the Pangani Estuary

Simulation of Tidal Currents

The hydrodynamic regime of the Pangani estuary is considered to be influenced by three natural forcing namely; the tidal currents, freshwater outflows from the Pangani river and the monsoon wind generated currents. The simulated tidal currents during the ebb tidal phase (Figs. 17 and 18), tended to flow radially, that is both eastwards, northwards and southwards up to at least during the first four hours. The radial flow pattern could be attributed to the funnel shape of the estuary. This is because the funneling effects enhance the magnitude and the direction of the tidal currents (Rao et al. 2011). On the upstream side of the estuary, the cross sectional area of the estuary is narrower compared to the estuarine mouth. Along the narrower parts of the estuary, the water would tend to flow at high speeds which would be reduced further downstream on the wider parts of the estuary, at the estuary mouth. The funnel like morphology of the estuary would therefore tend to induce a radial flow pattern towards the open sea.

The model simulation results showed that highest intensification of tidal currents were confined within a narrow zone located on the river mouth, while weaker tidal currents occurred further offshore and further upstream of the river mouth. Moreover tidal currents tended to be stronger on the northern coastal section of the river mouth adjacent to Pangani Town and Kigombe village than on the southern coastal section of the river mouth adjacent to Bweni village. The observed model simulated results are consistent with the observed pattern of shoreline erosion at Pangani (Shaghude 2004). However the study of Shaghude (2004) attributed most of the observed shoreline changes (particularly coastal erosion) to monsoonal wind generated waves. The present study revealed that apart from waves, the tidal currents were

also among the major contributing factors to the observed shoreline changes at Pangani. The present model simulated results further revealed that flooding of the estuary started from the southern parts before the northern parts, suggesting that there is a tidal phase difference between the southern parts of the estuary and the northern parts. This could probably be attributed to the observed difference of the bathymetry between the northern coastal section and southern coastal section of the investigated area.

The Dominant Forcing of the Pangani Estuary Hydrodynamics and SPM Fluxes

Deposition of SPM on the Pangani estuary preferentially occurred on the northern parts of the estuary than on the southern parts (Fig. 22). The observed low deposition of SPM on the southern parts of the estuary relative to the northern parts is probably due to the fact that the northward transport of SPM fluxes is more favored than the southward transport due to the dominance of the SE monsoon winds over the NE monsoon winds along the coast of Tanzania (Muzuka and Shaghude 2000; Shaghude et al. 2003). The relationship between SPM deposition and the hydrodynamic regime of estuaries has been studied by Wolanski et al. (1996), Uncles and Stephens (1997) and Azevedo et al. (2010). The results of the present study are consistent with the observations reported at Douro estuary where the change of estuarine hydrodynamics affected the dispersion of SPM originated from runoff (Azevedo et al. 2010). The estuarine hydrodynamics involve, the tidal currents, river discharge and wind regime; all of these affects the transport and dispersion pattern of SPM (Burchard 2008; Webster et al. 2014).

Although the model simulation in this study was based on the tidal currents, other studies (e.g. Flemer and Clamp 2006; Lane et al. 2007; Burchard 2008; Liu et al. 2009; Azevedo et al. 2010) showed that the variation of the river discharge also affects the deposition and dispersion of SPM in estuary. For instance Azevedo et al. (2010) showed that stable flow of the river discharge seem to be more effective on the dispersion of SPM compared to unstable flow. However, in the case of the Pangani estuary, the River forcing is relatively low, especially during the dry season. During the peak of the long rain season (in April) the River forcing cannot be neglected. The wind forcing is another important factor influencing the deposition of SPM. Lane et al. (2007) showed that the wind forcing tend to re-suspend the deposited SPM, bringing them back to the water column. In the present study, the observed preferential deposition of SPM on the northern parts of the estuary are being attributed to the dominance of the SE monsoon winds over the NE monsoon winds.

The Relationship between the Pangani Estuary Hydrodynamic Regime and Shoreline Changes and Deposition of Sediments

The funnel shaped nature of the Pangani Estuary, its orientation and the absence of a well-defined delta (depo-centre) are among the most important physical attributes characterizing the hydrodynamic regime of the Pangani estuary. The simulated model results revealed that the tidal currents were highly intensified proximal to the river mouth. Such hydrodynamic conditions would tend to accelerate shoreline erosion over time and would inhibit formation of the delta on the river mouth. Furthermore, the study of wind climate regime along the coast of Tanzania show that the coastal winds have intensified during the last three decade (Mahongo et al. 2012; Shaghude et al. 2012) suggesting that the wave climate regime have also changed over the last three decades. The intensification of waves could also inhibit the formation of a delta at the Pangani estuary. Finally, upstream anthropogenic activities associated with abstraction of river water by irrigation and impoundment of river water at Nyumba ya Mungu dam are also considered to have significant reduced the river sediment loads being discharged to the Pangani estuary. There is therefore no doubt that the present sea bottom morphology of the Pangani Estuary is being controlled by the hydrodynamic regime of the Pangani estuary.

The ebb currents seem to play a significant role in transporting the sediments brought by the Pangani River. The simulated model results revealed that the currents during the ebb tidal phase were very strong and with a general northward flow, approximately parallel to the shoreline. These currents are considered to play a significant role in shore erosion of the northern banks of the Pangani River mouth. In addition to tidal currents, Shaghude (2006) noted that the shore erosion on the northern banks of the Pangani River mouth was highly attributed by waves particularly during the NE monsoon season. The wind generated waves may also influence sediment re-suspension (Capo et al. 2006; Rostamkhani 2015).

The Long-Term Implication of the Observed Hydrodynamic Regime of the Pangani Estuary

The SPM fluxes per year at each station were estimated to determine the average deposition of SPM in the estuary (Fig. 23). The results indicated that approximate 872.6 kg/m²/year of SPM are being deposited to the estuary, of which 394 kg/m²/year are being deposited northwards (comprising stations 6 to 9), while 292 kg/m²/year are being deposited southwards (comprising stations 1 to 3) and 96.6 kg/m²/year (comprising stations 4 and 5) are being deposited at the middle of the river mouth.

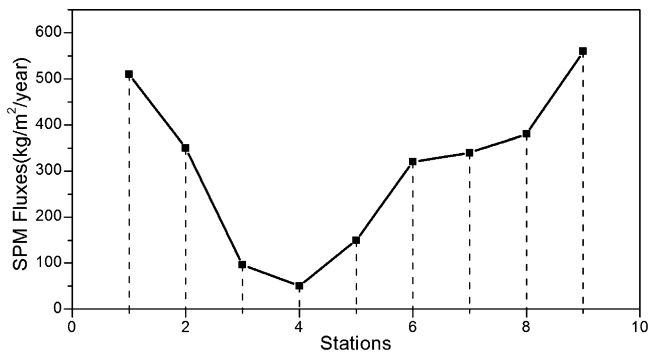


Fig. 23 SPM fluxes deposition per year in station 1–9 across the estuary mouth

The presented results suggest that in the long term, the SPM deposition pattern in the estuary mouth will significantly change the Pangani river mouth hydrodynamics regime from its present condition. The deposition of SPM fluxes which shows preferential deposition on the northern parts (station 6 to 9) would result to significant changes of the northern parts of the estuarine bottom topography. This could potentially lead to more turbulence conditions on the northern parts of the estuary as the incoming waves would tend to break as they approach the shallow estuarine topography. Marine vessels calling to the Pangani harbour (Town) could only access the harbour from the southern parts of the estuary. Thus if the current SPM deposition would persist for a long time marine vessels calling to Pangani harbour (Pangani Town) or marine vessels leaving the Pangani harbour must take the necessary precautions to ensure maximum safety.

Conclusion

The deposition of SPM in the Pangani Estuary showed a parabolic curve depositional pattern with maximum deposition located at about 3.3 km north or south of the central axis of the Estuary, and the minimum deposition occurring at the centre of the Estuary. The maximum SPM deposition occurred between May to August and the minimum deposition occurred from December to February. The spatial and temporal variation of SPM observed in Pangani Estuary was influenced by several factors including, monsoon wind, river discharge and tidal currents. The SPM deposition observed north or south of the Estuary was related with the seasonal pattern of the monsoon winds. Although deposition of SPM occurred at both the southern and northern parts of the estuary mouth, preferential deposition occurred on the northern parts, and this was attributed to the fact that the SE monsoon winds are stronger than NE monsoon winds (Newell 1959; Mahongo et al. 2012). The minimum deposition of SPM observed at the centre of the estuary was

influenced by a combination of tidal current and river discharge. Along the central axis of the estuary, water flows at relatively high speeds, thereby prohibiting the deposition of SPM. The study also have revealed that, approximately 872.6 kg/m²/year of SPM fluxes are being brought to the estuary: 394 kg/m²/year being transported northward, 292 kg/m²/year being transported southward and 96.6 kg/m²/year at the centre of the estuary. It implies that for a long run, the SPM deposition in the Pangani estuary will change the hydrodynamic regime from its present condition.

In addition, the model simulation showed that the strongest tidal currents in the Pangani Estuary occurred on the northern coastal section of the river mouth adjacent to Pangani Town and Kigombe village compared to the southern coastal section of the river mouth adjacent to Bweni village. The flooding tidal currents from the northern parts of the river mouth were lagging behind the flooding tidal current from the southern parts of the river mouth. The ebb tidal currents that originated from the inner part of the estuary tended to flow radially soon after reaching the river mouth. The radial flow pattern of the tidal currents seemed to be influenced by the funnel shape nature of the estuary. The intensification of the tidal currents on the river mouth tended to intensify shoreline retreat and inhibited the formation of a delta off the Pangani river mouth. Apart from the observed natural factors the hydrodynamic regime of the Pangani estuary are also influenced by the upstream anthropogenic activities associated with abstraction of river water by irrigation and impoundment of river water at Nyumba ya Mungu dam.

Acknowledgement We are grateful to anonymous reviewers for their constructive comments that enabled this paper to be as it is. We are also grateful to the divers and technicians of the Institute of Marine Sciences for their assistance in fieldwork. This work described was funded by Western Indian Ocean Regional Initiative in Marine Sciences and Education (WIO-RISE)

References

- ASCLME (2012) National marine ecosystem diagnostic analysis (MEDA): Agulhas and Somali Current Large Marine Ecosystems Project. Available at http://asclme.org/report2013/national%20MEDA/mozambique/_MozambiqueMEDAProof.pdf
- Azevedo IC, Bordalo AA, Duarte PM (2010) Influence of river discharge patterns on the hydrodynamics and potential contaminant dispersion in the Douro estuary (Portugal). *Water Res* 44:3133–3146
- Bailey A, Chase TN, Cassano JJ, Noone D (2011) Changing temperature Inversion characteristics in the U.S Southwest and relationship to largescale atmospheric circulation. *J Appl Meteor Climatol* 50:1307–1323
- Bilgili M, Prochi JA, Lynch DR, Smith WK, Smith MR (2005) Estuary or ocean exchange and tidal mixing in a Gulf of Marine Estuary, a Lagranging modeling study. *Estuar Coast Shelf Sci* 65:607–624

- Burchard H (2008) Combined effects of wind tide and horizontal density gradients on stratification in estuaries and coastal seas. *J Phys Oceanogr* 39:2117–2136
- Capo S, Sottolichio A, Brenon I, Gastaing P, Ferry L (2006) Morphology, hydrography and sediments dynamics in mangrove estuary: the Konkoure estuary. *Guinea Mar Geol* 230:199–215
- Carmeron WM, Pritchard D (1963) Estuaries. In: Hill MN (ed) *The sea*, vol 2. Wiley, New York, pp 306–324
- Comerma E, Espino M, Sánchez-Arcilla A, González M (2002) Forecasting oil pollution in harbour engineering. In: Proceedings of the 29th international conference on coastal engineering. American Society of Civil Engineers (ASCE), pp 1242–1253
- Cuff WR, Tomczak M (1983) Synthesis and modelling of intermittent estuaries. Springer, Berlin/Heidelberg/New York
- DHI (2007) MIKE 21: sediment transport and morphological modelling – user guide. DHI Water and Environment, Hørsholm, p 388
- Duck RW, Wewetzer SFK (2001) Impact of frontal system on estuarine sediment and pollutants dynamics. *Sci Total Environ* 266:23–31
- Duvail S, Hammerlynk O (2007) Rufiji river flood: plague or blessing? *Int J Biometeorol* 52:32–42
- Duarte P (2008) A three dimensional hydrodynamic model implemented with ecodynamo Available at: <https://bdigital.ufp.pt/dspace/handle/10284/834>
- English S, Wilkinson C, Baker V (1994) Survey manual for tropical marine resources. Australian Institute of Marine Sciences, Townsville, p 358
- Flemer DA, Clamp MA (2006) What is the future given nutrient over-enrichment, freshwater diversion and low flows. *Mar Pollut Bull* 52:247–258
- Francis J, Wagner GM, Mvungi A, Ngwale J, Sallema R (2001) Tanzania national report, phase I: integrated problem analysis. Unpublished report: GEF MSP Sub-Saharan Africa Project on Development and Protection of the Coastal and Marine Environment in Sub-Saharan Africa, 60 pp
- Garcia-Reyes M, Mayorga-Adame G, Moulton MR, Nadeau PC (2009) Modelling of the Zanzibar channel. Unpublished report, Institute of Marine Sciences, Zanzibar., 13 p
- Gerritsen H, Robert JV, Theo VK, Andrew L, Boon JG (2000) Suspended sediment modeling in a shelf sea (North Sea). *Coast Eng* 41:317–352
- Ghimire S (2013) Application of 2D hydrodynamic model for assessing flood risk from extreme storm events. *Climate* 1:148–162
- Gisen JIA, Savenije HHG, Njzink RC (2015) Revised predictive equations for salt intrusion modelling in estuaries. *Hydrol Earth Syst Sci Discuss* 12:739–770
- Gleizona P, Punta AG, Lyonsb MG (2003) Modelling hydrodynamics and sediment flux within a macrotidal estuary: problems and solutions. *Sci Total Environ* 314–316:589–597
- Gritfull M, Fontán A, Ferrer L, Manuel M, Espino GM (2009) 3D hydrodynamic characterisation of a meso-tidal harbour: the case of Bilbao (northern Spain). *Coast Eng* 56:907–918
- Hafslund AS (1980) Stiegler's Gorge power and flood control development. Project planning. Unpublished report volume 1 Oslo Report to RUBANDA
- Hu KL, Ding PX, Wang ZB, Yang SL (2009) A 2D/3D hydrodynamic and sediment transport model for the Yangtze Estuary, China. *J Mar Syst* 77:114–136
- IUCN (2003) Eastern African Programme. The Pangani River basin: a situation analysis, The World Conservation Union; ScanHouse Press Ltd, Nairobi. p 104
- James ID (2002) Modelling pollution dispersion, the ecosystem and water quality in coastal water: a review. *Environ Model Software* 91:99–164
- Jay DA, Leffler K, Diefenderfer HL, Borde AB (2014) Tidal-fluvial and Estuarine processes in the lower Columbia River: I, a long-channel water level variations, Pacific ocean to Bonneville Dam. *Estuar Coasts* 38:415–433. doi:10.1007/s12237-014-9819-0
- Kabanda TA, Jurry MR (1999) Inter-annual variability of short rains over northern Tanzania. *Climate Res* 13:231–241
- Kijazi AL, Reason CJC (2009) Analysis of the 2006 floods over Northern Tanzania. *Int J Climatol* 29:955–970
- Kregting L, Elsaber B (2014) A hydrodynamic modelling framework for Strangford Lough Part 1: tidal model. *J Mar Sci Eng* 2:46–65
- Lane RR, Day JW, Marx BD, Reyes E, Hyfield E, Day JN (2007) The effects of riverine discharge on temperature salinity suspended sediments and chlorophyll a in a Mississippi delta estuary measured using a flow-through system. *Estuar Coast Shelf Sci* 74:145–154
- Liu WC, Chen WB, Cheng RT, Hsu MH, Kuo AY (2009) Modeling the influence of river discharge on salt intrusion and residual circulation in Danshuei River estuary, Taiwan. *Cont Shelf Res* 27:900–921
- Long JW (2009) Modeling shallow-water hydrodynamics: rotations, rips, and rivers: a dissertation submitted to Oregon State University
- Lopes JF, Dias JM, Cardoso AC, Silva CIV (2005) The water quality of Ria de Aveiro lagoon, Portugal: from the observations to the implementation of a numerical model. *Mar Environ Res* 60:594–628
- Mahongo SB, Shaghude YW (2014) Modelling the dynamic of the Tanzanian Coastal water. *J Oceanogr Mar Sci* 5:1–7
- Mahongo SB, Francis J, Osima SE (2012) Wind patterns of coastal Tanzania: their variability and trends. *West Indian Ocean J Mar Sci* 10:107–120
- Mayorga-Adame CG (2007) Ocean circulation of the Zanzibar channel: a modeling approach. IMS, Zanzibar, p 8
- McSweeney C, New M, Lizeano G (1998) Tanzania model projection of climate changes: report UNDP climate change country Profile. <http://country-profiles.Geog.ox.ac.uk>
- Mrema LE (2012) Characteristics of water circulation in Mnazi Bay, Tanzania. Msc. thesis, University of Dar es Salaam
- Muzuka ANN, Shaghude YW (2000) Grain size distribution along Msasani beach, north of Dar es Salaam harbour. *J Afr Earth Sci* 30:417–426
- Muzuka ANN, Dubi AM, Muhando CA, Shaghude YW (2010) Impact of hydrographic parameters and seasonal variation in sediment fluxes on coral status at Chumbe and Bawe reefs, Zanzibar, Tanzania. *Estuar Coast Shelf Sci* 89:137–144
- Newell BS (1959) The hydrography of British East African coastal waters. *Col Off Fish Pubs Lond* 12:1–18
- Priya KL, Jegathambel P, James EJ (2012) Hydrodynamic modelling of estuaries-A-state-of-art. *Int J Environ Sci* 3:223–240
- Rao PV, Shynu R, Kessarkar PM, Sundar D, Michael GS, Navekar T, Blossom V, Mehra P (2011) Suspended sediment dynamics on a scale in the Mandovi and Zuari estuaries, Central west coast of India. *Estuar Coast Shelf Sci* 91:78–86
- Rostamkhani HM (2015) A novel approach to flow and sediment transport estimation in estuaries and bays. http://pdxscholar.library.pdx.edu/open_access_etds
- Smagorinsky J (1963) General circulation experiment with the primitive equations. *Monthly Weather Rev* 91:99–164
- Shaghude YW (2004) Shore Morphology and sediment characteristics south of Pangani River, coastal Tanzania. *West Indian Ocean J Mar Sci* 3:93–104
- Shaghude YW (2006) Review of water resource exploitation and land use pressure in the Pangani river basin. *West Indian Ocean J Mar Sci* 5:195–207
- Shaghude YW, Wannas KO, Mahongo SB (2003) Biogenic assemblage and hydrodynamic setting of the tidally dominated reef platform sediments of Zanzibar channel. *West Indian Ocean J Mar Sci* 1:107–116
- Shaghude YW, Mburu JW, Nyandwi N, Magori C, Ochiewo J, Sanga I, Arthurton R (2012) Beach sand supply and transport at Kunduchi in Tanzania and Bamburi in Kenya. *West Ind Ocean J Mar Sci* 11:135–154

- Silva PD, Lisboa PV, Fernandes EH (2015) Changes on fine sediments dynamic of the Port of Rio Grande expansion. *Adv Geosci* 39:123–127
- Sotthewes W (2008) Forcing the salinity distribution in the Pangani estuary. Final report, Delft University of Technology, p 85. Available at www.citg.tudelft.nl/fileadmin/Faculteit/.../Sothewes_2008.pdf
- Strickland JDH, Parsons TR (1972) A practical handbook of seawater analysis. Bulletin 167, 2nd ed. Fisheries Research Board of Canada, Ottawa, 310 p
- Tanaka A, Deleersnijder E (1996) Three-dimensional Island Wakes in the field, Laboratory experiments and numerical models. *Continental Shelf Res* 16:1437–1452
- Timbadiya PV, Patel PL, Porey PD (2013) One dimensional hydrodynamic modelling of flooding and stage hydrographs in the lower Tapi River in India. *Curr Sci* 106:708–716
- Uncles RJ, Stephens JA (1997) The freshwater-saltwater interface and its relationship to the turbidity maximum in the Famar estuary, United Kingdom. *Estuaries* 16:126–141
- UNEP (1998) Maziwi Island off Pangani (Tanzania) history of its destruction and possible causes: UNEP regional seas report and studies number 139. Available at <http://iwlearn.net/publications/regional-seas-reports-and-studies-no-139/view>
- Webster T, McGuigan K, Collins K, McDonald C (2014) Integrated river and coastal hydrodynamic flood risk mapping of the LaHave river estuary and town of Bridgewater, Nova Scotia, Canada. *Water* 6:517–547
- Welcomme RL (1972) The inland waters of Africa. Les eaux interieures d’Afrique-CIFA teach pap/Doc. Tech. CPCA 1:117p
- Wolanski E, Asaeda T, Tanaka A, Deleersnijder E (1996) Three-dimensional island wakes in the field, Laboratory experiments and numerical models. *Contl Shelf Res* 16:1437–1452
- Zacharias I, Gianni A (2008) Hydrodynamic and dispersion modeling as a tool for restoration of coastal ecosystems. Application to a re-flooded lagoon. *Environ Model Software* 23:751–767
- Zheng-Gang J (2008) Hydrodynamic and water quality: modelling rivers, lakes and estuaries. Wiley, Hoboken, 702 pp
- Zorita E, Tilya FF (2002) Rainfall in Northern Tanzania in March- May Season (long rains) and its links to large scale climate forcing. *Climate Res* 20:31–40